RESEARCH ARTICLE | JUNE 07 2023

A data-driven approach to solving a 1D inverse scattering problem

Tristan van Leeuwen ; Andreas Tataris

AIP Advances 13, 065310 (2023)
https://doi.org/10.1063/5.0154182

A data-driven approach to solving a 1D inverse scattering problem

Cite as: AIP Advances 13, 065310 (2023); doi: 10.1063/5.0154182
Submitted: 13 April 2023 • Accepted: 12 May 2023 •
Published Online: 7 June 2023

Tristan van Leeuwen[1,2a)] and Andreas Tataris[2]

AFFILIATIONS

[1] Centrum Wiskunde and Informatica, Amsterdam, The Netherlands
[2] Utrecht University, Utrecht, The Netherlands

[a)] **Author to whom correspondence should be addressed:** t.van.leeuwen@cwi.nl

ABSTRACT

In this paper, we extend a recently proposed approach for inverse scattering with Neumann boundary conditions [Druskin *et al.*, Inverse Probl. **37**, 075003 (2021)] to the 1D Schrödinger equation with impedance (Robin) boundary conditions. This method approaches inverse scattering in two steps: first, to extract a reduced order model (ROM) directly from the data and, subsequently, to extract the scattering potential from the ROM. We also propose a novel data-assimilation (DA) inversion method based on the ROM approach, thereby avoiding the need for a Lanczos-orthogonalization (LO) step. Furthermore, we present a detailed numerical study and A comparison of the accuracy and stability of the DA and LO methods.

I. INTRODUCTION

Inverse scattering appears in many applications, including medical imaging, non-destructive testing, and geophysical exploration.[1] While acquisition setups differ at their core, all these inverse problems involve a wave equation and require an estimation of its variable coefficients from boundary data. Approaches to solving the resulting inverse problem can be classified as either *direct* or *indirect* methods. The direct methods originate in classical inverse scattering theory and rely on formulating a linear relation between scattering data and medium coefficients; see, e.g., Ref. 2. The indirect methods formulate a non-linear data-fitting problem that needs to be solved iteratively.[3]

The indirect methods have been extensively investigated in the past decades with major breakthroughs addressing the computational cost and the non-linearity of the data-fitting problem.[4,5] Still, the non-linearity remains a major challenge for this approach.

The direct methods have recently attracted renewed attention, as a means of addressing this non-linearity.[6–8] A recent development is the use of data-driven reduced-order models (ROMs) for solving the inverse scattering problem.[9] In this approach, a reduced-order model is computed directly from the data via an orthogonalization procedure, and from this, the underlying state is estimated. From the estimated state, the corresponding coefficient is estimated by solving a Lippmann–Schwinger integral equation. Challenges for this approach include the sensitivity of the orthogonalization approach to noise in the measurements.

The ROM-based approach has been applied in various settings, including time-domain wave propagation, see, e.g., Ref. 10, and frequency-domain diffusion processes, see Ref. 9. As a first step toward extending this procedure to frequency-domain wave problems, we extend the approach to a 1D Schrödinger equation with impedance boundary conditions. It turns out that both reflection and transmission measurements are needed to compute the ROM from the data. Furthermore, we propose an alternative approach to the orthogonalization-based state estimation approach described in Ref. 9. To study the accuracy and stability properties of the resulting methods, we present numerical experiments.

This paper is organized as follows. First, we review the forward problem and present the relations between the boundary data and required ROM matrices. Then, we discuss the two-step approach to solve the inverse problem: state estimation and subsequent estimation of the coefficients from the state. We then present numerical experiments to illustrate the accuracy and stability of both methods on noisy data. We conclude this paper with a brief summary of the main findings and a discussion on further work.

II. THE FORWARD PROBLEM

Consider the 1D Schrödinger equation,

$$-u''(x;k) + q(x)u(x;k) - k^2 u(x;k) = 0, \quad x \in (0,1), \tag{1}$$

with boundary conditions,

$$u'(0;k) + \imath k u(0;k) = 2\imath k, u'(1;k) - \imath k u(1;k) = 0, \tag{2}$$

which corresponds to an incoming plane wave from $-\infty$. The scattering potential q is assumed to have compact support in (0,1). The measurements are given by

$$f(k) = u(0;k), \quad g(k) = u(1;k). \tag{3}$$

Well-posedness of this forward problem has been well-established (at least when q is continuous) since the boundary value problem can be transformed to the Lippmann–Schwinger integral equation; see, e.g., Ref. 11.

A. A reduced-order model

The point of departure for the ROM-based approach is the weak formulation of (1) and (2),

$$\langle u', \phi' \rangle + \langle qu, \phi \rangle - k^2 \langle u, \phi \rangle - \imath k \Big(f(k)\overline{\phi(0)} + g(k)\overline{\phi(1)} \Big) = -2\imath k \overline{\phi(0)} \quad \forall\, \phi, \tag{4}$$

where $\langle \cdot, \cdot \rangle$ denotes the standard inner product in $L^2(0,1)$ and $\bar{\cdot}$ denotes the complex conjugation.

Representing the solution as a linear combination of solutions $\{u_i\}_{i=0}^{m-1}$ with $u_i \equiv u(\cdot\,; k_i)$, and using the same as test functions, the resulting system matrices are defined, correspondingly,

$$S_{ij} = \langle u_j', u_i' \rangle + \langle q u_j, u_i \rangle, \tag{5}$$

$$M_{ij} = \langle u_j, u_i \rangle, \tag{6}$$

$$B_{ij} = f_j \overline{f_i} + g_j \overline{g_i}, \tag{7}$$

and right-hand side,

$$b_i = -2\imath k \overline{f_i}. \tag{8}$$

Correspondingly, the approximate solution is then given by

$$\widetilde{u}(x;k) = \sum_{i=0}^{m-1} c_i(k) u_i(x), \tag{9}$$

with the coefficients obeying

$$\big(S - k^2 M - \imath k B\big)\mathbf{c}(k) = \mathbf{b}(k). \tag{10}$$

We refer the reader to Refs. 12–15 for the discussion regarding the approximation error of such ROM approximations.

The main feature making this approach useful for solving the inverse problem is that the system matrices can be computed from the data directly, as per the following lemma.

Lemma 1. The ROM system matrices S, M [Eqs. (5) and (6)] are given in terms of the boundary data $\{f_i\}_{i=0}^{m-1}$ and $\{g_i\}_{i=0}^{m-1}$ [Eq. (3)] as

$$S_{ij} = \imath \left(\frac{k_i k_j B_{ij}}{k_i - k_j} - 2 \frac{k_j^2 k_i f_j + k_i^2 k_j \overline{f_i}}{k_i^2 - k_j^2} \right), \quad i \neq j,$$

$$S_{ii} = k_i^2 \big(\Re(f_i)\Im(f_i') - \Im(f_i)\Re(f_i') + \Re(g_i)\Im(g_i') - \Im(g_i)\Re(g_i') \big) - \Im(f_i') - \Im(f_i)/k_i.$$

$$M_{ij} = \imath \left(\frac{B_{ij}}{k_i - k_j} - 2 \frac{k_i f_j + k_j \overline{f_i}}{k_i^2 - k_j^2} \right), \quad i \neq j,$$

$$M_{ii} = \Re(f_i)\Im(f_i') - \Im(f_i)\Re(f_i') + \Re(g_i)\Im(g_i') - \Im(g_i)\Re(g_i') - \Im(f_i') + \Im(f_i)/k_i.$$

The proof of this lemma can be found in the Appendix.

Remark 1. From the Proof of Lemma 1, we see that $c_i(k_j) = \delta_{ij}$. Thus, we have $\widetilde{u}(k_i) = u_i$.

III. THE INVERSE PROBLEM

The inverse problem is now to retrieve the scattering potential, q, from boundary measurements at wave numbers $\{k_i\}_{i=0}^{m-1}$,

$$\mathbf{f} = (f(k_0), f(k_1), \ldots, f(k_{m-1}))$$

and

$$\mathbf{g} = (g(k_0), g(k_1), \ldots, g(k_{m-1})).$$

This is achieved in a two-step procedure. First, the states $\{u_i\}_{i=0}^{m-1}$ are estimated from the data, and subsequently, the scattering potential, q, is estimated from these approximated states $\{\widetilde{u}_i\}_{i=0}^{m-1}$.

A. Estimating the state

As outlined in Sec. II, we can compute the *coefficients* in (9) directly from the data by solving (10) with $S, M, B, \mathbf{b}$ obtained from the boundary data as stated in Lemma 1. Since the basis $\{u_i\}_{i=0}^{m-1}$ needed to evaluate (9) is unknown, however, we need to use a different basis. The basic idea is to use states $\{u_i^{(0)}\}_{i=0}^{m-1}$ corresponding to a given $q^{(0)}$ instead. It is tempting to directly replace u_i in (9) by $u_i^{(0)}$ corresponding to a reference scattering potential $q^{(0)}$. However, this will not work as it would yield $\widetilde{u}(x;k_i) = u_i^{(0)}(x)$, see Remark 1. Below, we discuss two alternatives.

1. Lanczos orthogonalization

The authors of Ref. 9 propose to use an orthogonalization procedure as follows. They first apply the M-orthogonal Lanczos procedure to $M^{-1}S$, which yields matrices $Q \in \mathbb{C}^{m\times r}$ and $T \in \mathbb{C}^{r\times r}$, where $r \leq m$, satisfying

$$Q^* S Q = T, \quad Q^* M Q = I.$$

ALGORITHM 1. Overview of the two-step inversion procedure to estimate the states and scattering potential from boundary data.

Input: reference $q^{(0)}$, data f, g at wavenumbers $\{k_i\}_{i=0}^{m-1}$, regularisation parameters $((\epsilon, \alpha)$ or $(\rho, \alpha))$
Output: reconstructed states $\{\widetilde{u}_i\}_{i=0}^{m-1}$ and scattering potential $\widetilde{q}$.

Step 1: state estimation

Compute ROM-matrices M, S, B according to Lemma 1

Compute reference states $\{u_i^{(0)}\}_{i=0}^{m-1}$ corresponding to $q^{(0)}$.

Compute approximate states $\{\widetilde{u}_i\}_{i=0}^{m-1}$ at wavenumbers $\{k_i\}_{i=0}^{m-1}$ according to the LO or DA procedures (outlined in sections 3.1.1, 3.1.2 resp.)

Step 2: estimating the scattering potential

Reconstruct the scattering potential $\widetilde{q}$ according to the procedure outlined in Sec. 3.1.3

Remark 2. In practice, we replace M by $M + \epsilon I$ for some $\epsilon > 0$ to ensure it is invertible and to stabilize the Lanczos procedure.

The ROM approximation of the state (9) can then be expressed as

$$\widetilde{u}(x;k) = \sum_{i=0}^{m-1} c_i^{\mathrm{LO}}(k) v_i(x), \tag{11}$$

with the coefficients $\mathbf{c}^{\mathrm{LO}}(k)$ satisfying

$$\left(T - k^2 I - \imath k Q^* B Q\right)\mathbf{c}^{\mathrm{LO}}(k) = Q^*\mathbf{b}(k), \tag{12}$$

and where $\{v_i\}_{i=0}^{r-1}$ defined by

$$v_j = \sum_{i=0}^{m-1} Q_{ij} u_i,$$

is an *orthogonal* (w.r.t. the regular L^2-inner product) basis for the span of $\{u_i\}_{i=0}^{m-1}$. Because we do not have access to the states $\{u_i\}_{i=0}^{m-1}$ in practice, we cannot form the orthogonal basis $\{v_i\}_{i=0}^{r-1}$. Instead, we replace it by $\{v_i^{(0)}\}_{i=0}^{r-1}$, as

$$v_j^{(0)} = \sum_{i=0}^{m-1} Q_{ij}^{(0)} u_i^{(0)},$$

where the states $u_i^{(0)}$ are the solutions for a reference scattering potential $q^{(0)}$ and $Q^{(0)}$ is obtained by applying the Lanczos procedure to the corresponding system matrices. The resulting approximation of the state is then given by

$$\widetilde{u}^{\mathrm{LO}}(x;k) = \sum_{i=0}^{m-1} c_i^{\mathrm{LO}}(k) v_i^{(0)}(x). \tag{13}$$

2. Data assimilation

An alternative approach is inspired by Ref. 16 and sets up an overdetermined system of equations, which ensures that the resulting estimate of the internal solution closely matches the data. We

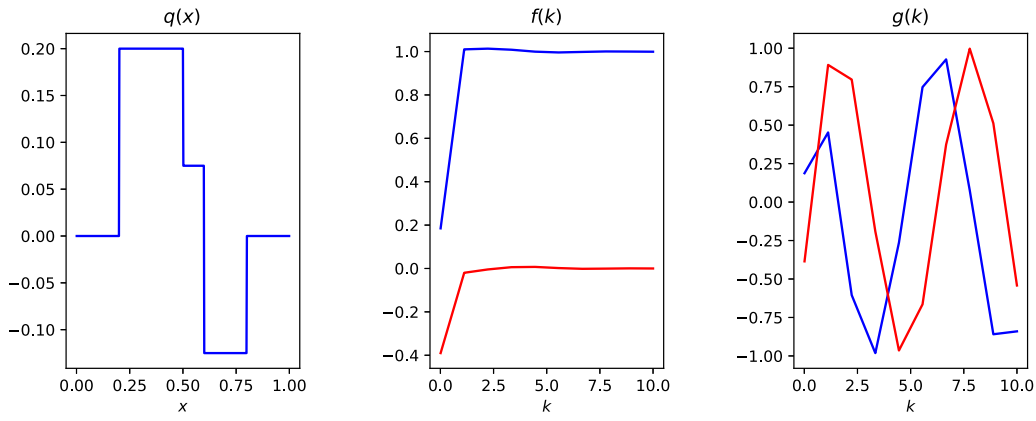

FIG. 1. From left to right, the scattering potential q, the real (blue) and imaginary (red) part of the reflection data, f, and the real and imaginary part of the transmission data, g.

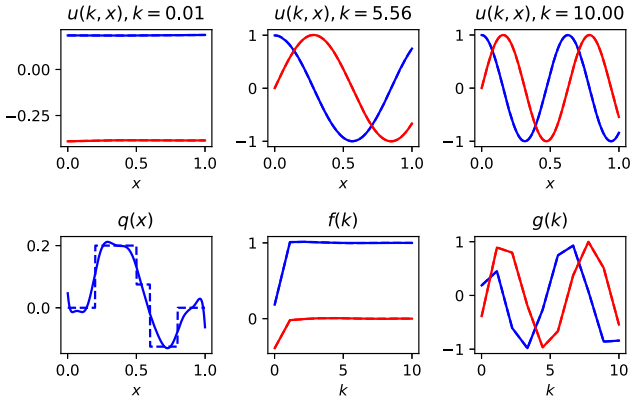

FIG. 2. Results using the true state to reconstruct the scattering potential. The top row shows the (reconstructed) states (solid) used in the subsequent step to estimate the scattering potential as well as the true states (dashed). In the second row, we see the reconstructed scattering potential (solid) and the corresponding data. The real part of the quantities is shown in blue, while the imaginary part is shown in red.

directly define the approximated state in terms of the reference solutions,

$$\widetilde{u}^{\mathrm{DA}}(x;k) = \sum_{i=0}^{m-1} c_i^{\mathrm{DA}}(k) u_i^{(0)}(x),$$

where the coefficients $\mathbf{c}^{\mathrm{DA}}(k)$ are obtained by solving the following least-squares problem:

$$\mathbf{c}^{\mathrm{DA}}(k) = \arg\min_{\mathbf{c}} \left\| \begin{pmatrix} S - k^2 M - \imath k B \\ \rho \mathbf{f}^{(0)^T} \\ \rho \mathbf{g}^{(0)^T} \end{pmatrix} \mathbf{c} - \begin{pmatrix} \mathbf{b}(k) \\ \rho f(k) \\ \rho g(k) \end{pmatrix} \right\|_2, \tag{14}$$

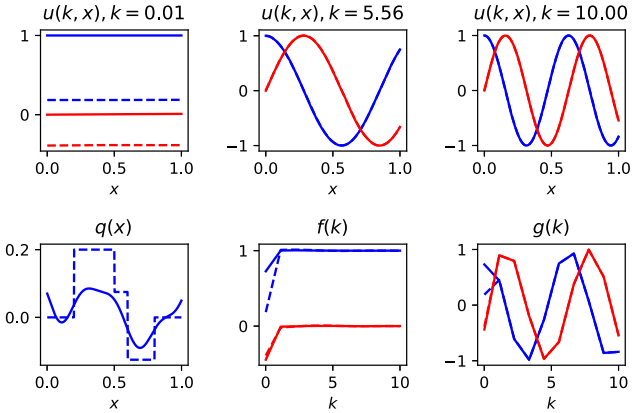

FIG. 3. Results using the reference state to reconstruct the scattering potential (i.e., the Born approximation). The top row shows the (reconstructed) states (solid) used in the subsequent step to estimate the scattering potential as well as the true states (dashed). In the second row, we see the reconstructed scattering potential (solid) and the corresponding data. The real part of the quantities is shown in blue, while the imaginary part is shown in red.

where $\rho > 0$ is a penalty parameter controlling the trade-off between data-fit and model-fit. Note that we can readily setup this least-squares problem for $k \in \{k_i\}_{i=0}^{m-1}$ since the required data $f(k_i)$, $g(k_i)$ for the right-hand-side is measured. If we want to evaluate this approximation for $k \notin \{k_i\}_{i=0}^{m-1}$, we need to interpolate the data first.

For $\rho = 0$, we will obtain $\widetilde{u}^{\mathrm{DA}}(x;k_i) = u_i^{(0)}(x)$, and this will not yield any additional information on the true state. For $\rho > 0$, the additional terms aim to ensure that $\widetilde{u}^{\mathrm{DA}}(0;k) \approx f(k)$ and $\widetilde{u}^{\mathrm{DA}}(1;k) \approx g(k)$. This is a fundamental difference with the Lanczos-based approach, where data-fit is not enforced at all.

B. Estimating the scattering potential

Using the weak formulation of the differential equation, we obtain a Lippmann–Schwinger-type equation for the scattering potential,

$$f(k) - f^{(0)}(k) = -\frac{1}{2\imath k} \int_0^1 u^{(0)}(x;k) u(x;k) (q(x) - q_0(x)) \mathrm{d}x. \tag{15}$$

Representing q in terms of a suitable basis and enforcing the equation for wavenumbers $\{k_i\}_{i=0}^{m-1}$ yields a system of equations. In practice, we replace u by its approximation $\widetilde{u}$ and solve it in a least-squares sense to obtain an estimate of the scattering potential,

$$\min_{\mathbf{q}} \|K\mathbf{q} - (\mathbf{f} - \mathbf{f}^{(0)})\|_2^2 + \alpha \|\mathbf{q}\|_2^2. \tag{16}$$

Remark 3. Note that replacing u by $\widetilde{u}$ in (15) induces an error in K. To explicitly account for this, a Total Least-Squares (TLS) formulation (see e.g., Ref. 17 for its use in inverse scattering) might be beneficial.

IV. NUMERICAL RESULTS

The inversion procedure consists of two steps: state estimation and estimation of the scattering potential from the states. For

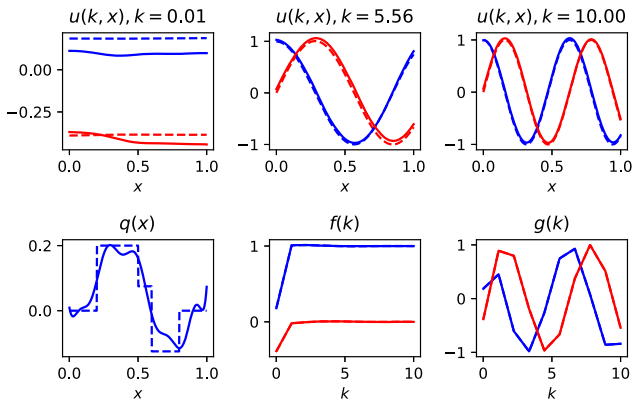

FIG. 4. Results using the LO approach on noiseless data. The top row shows the (reconstructed) states (solid) used in the subsequent step to estimate the scattering potential as well as the true states (dashed). In the second row, we see the reconstructed scattering potential (solid) and the corresponding data. The real part of the quantities is shown in blue, while the imaginary part is shown in red.

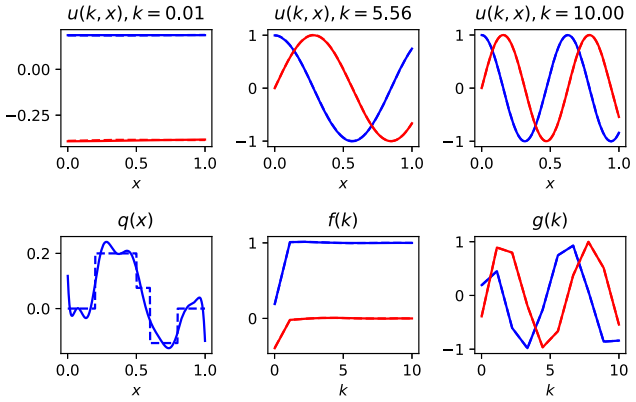

FIG. 5. Results using the DA approach on noiseless data. The top row shows the (reconstructed) states (solid) used in the subsequent step to estimate the scattering potential as well as the true states (dashed). In the second row, we see the reconstructed scattering potential (solid) and the corresponding data. The real part of the quantities is shown in blue, while the imaginary part is shown in red.

the first step, we use either the Lanczos orthogonalization approach (LO) with parameter ϵ or the data-assimilation approach (DA) with parameter ρ. With the approximated states, the scattering potential is then estimated by solving the regularized Lippmann–Schwinger equation, with parameter α. This two-step algorithm is outlined in Algorithm 1. Implementation of the described method is fairly straightforward. The code used to produce these results is available at https://github.com/ucsi-consortium/1DInverseScatteringROM.

A. Experimental settings

To illustrate the methods, we use the scattering potential depicted in Fig. 1. The data are obtained by numerically solving the Schrödinger equation for $m = 10$ equispaced wave numbers in the interval (0,10).

B. Benchmark results

As a benchmark, we reconstruct the scattering potential using the approach described in Sec. III B using the true states (as the ideal setting) and the reference states for $q^{(0)}(x) = 0$ (which corresponds to the Born approximation). The results are shown in Figs. 2 and 3. Even using the true states, we do not obtain a perfect reconstruction of the scattering potential due to the band-limited nature of the data. Furthermore, the inferior result obtained using the Born approximation underlines the need for non-linear inversion.

C. Noiseless data

Next, we present the results yielded by the (LO) and (DA) methods for noise-free data in Figs. 4 and 5, respectively. We observe that the DA method gives slightly more accurate reconstructions of the states. The corresponding reconstructed scattering potentials are slightly different, but there seems to be little difference in the accuracy of the reconstructions.

D. Noisy data

In this subsection, we compare the methods on noisy data. In particular, we add i.i.d. normally distributed noise to the data with mean zero and variance σ^2. The parameters ϵ, ρ, α are chosen to yield the best approximation (as measured by the L^2 error between the reconstructions and the ground truth, averaged over 100 realizations of the noise). The corresponding plots showing the dependence of the error on the parameters are included in the Appendix. In Table I, we summarize the results for varying σ. The corresponding plots are shown in Fig. 6. As expected, the noise influences the reconstruction of the state and consequently the reconstruction of the scattering potential. Overall, we see that the DA method gives superior estimates of the state. In terms of the scattering potential, there is no significant difference between both methods, however, for moderate noise levels, the DA method gives more stable results with a much smaller variance in the error.

TABLE I. Comparison between the relative errors in reconstructed states and scattering potential for both methods. We report the average and standard deviation over 100 realizations of the noise.

σ	Method	Parameters	Error in u	Error in q
10^{-6}	LO(ϵ,α)	$(10^{-3},10^{-3})$	$1.5\cdot10^{-1}$ $(1.6\cdot10^{-3})$	$4.7\cdot10^{-1}$ $(3.2\cdot10^{-3})$
	DA(ρ,α)	$(10^{-2},10^{-4})$	$6.1\cdot10^{-3}$ $(1.4\cdot10^{-5})$	$3.9\cdot10^{-1}$ $(2.3\cdot10^{-3})$
10^{-5}	LO(ϵ,α)	$(10^{-2},10^{-3})$	$1.5\cdot10^{-1}$ $(5.3\cdot10^{-4})$	$4.6\cdot10^{-1}$ $(2.3\cdot10^{-3})$
	DA(ρ,α)	$(10^{-1},10^{-3})$	$6.1\cdot10^{-3}$ $(3.0\cdot10^{-5})$	$4.5\cdot10^{-1}$ $(2.8\cdot10^{-3})$
10^{-4}	LO(ϵ,α)	$(10^{-2},10^{-2})$	$1.8\cdot10^{-1}$ $(1.5\cdot10^{-1})$	$5.7\cdot10^{-1}$ $(1.4\cdot10^{-1})$
	DA(ρ,α)	$(10^{-1},10^{-2})$	$6.2\cdot10^{-3}$ $(3.4\cdot10^{-4})$	$5.3\cdot10^{-1}$ $(3.2\cdot10^{-3})$
10^{-3}	LO(ϵ,α)	$(10^{-1},10^{-2})$	$2.1\cdot10^{-1}$ $(1.2\cdot10^{-1})$	$6.2\cdot10^{-1}$ $(1.3\cdot10^{-1})$
	DA(ρ,α)	$(10^{0},10^{-2})$	$6.4\cdot10^{-3}$ $(7.0\cdot10^{-4})$	$6.0\cdot10^{-1}$ $(5.9\cdot10^{-2})$
10^{-2}	LO(ϵ,α)	$(10^{-1},10^{-1})$	$2.6\cdot10^{-1}$ $(7.1\cdot10^{-1})$	$9.2\cdot10^{-1}$ $(9.4\cdot10^{-2})$
	DA(ρ,α)	$(10^{1},10^{-1})$	$1.4\cdot10^{-2}$ $(4.4\cdot10^{-3})$	$9.2\cdot10^{-1}$ $(9.0\cdot10^{-2})$

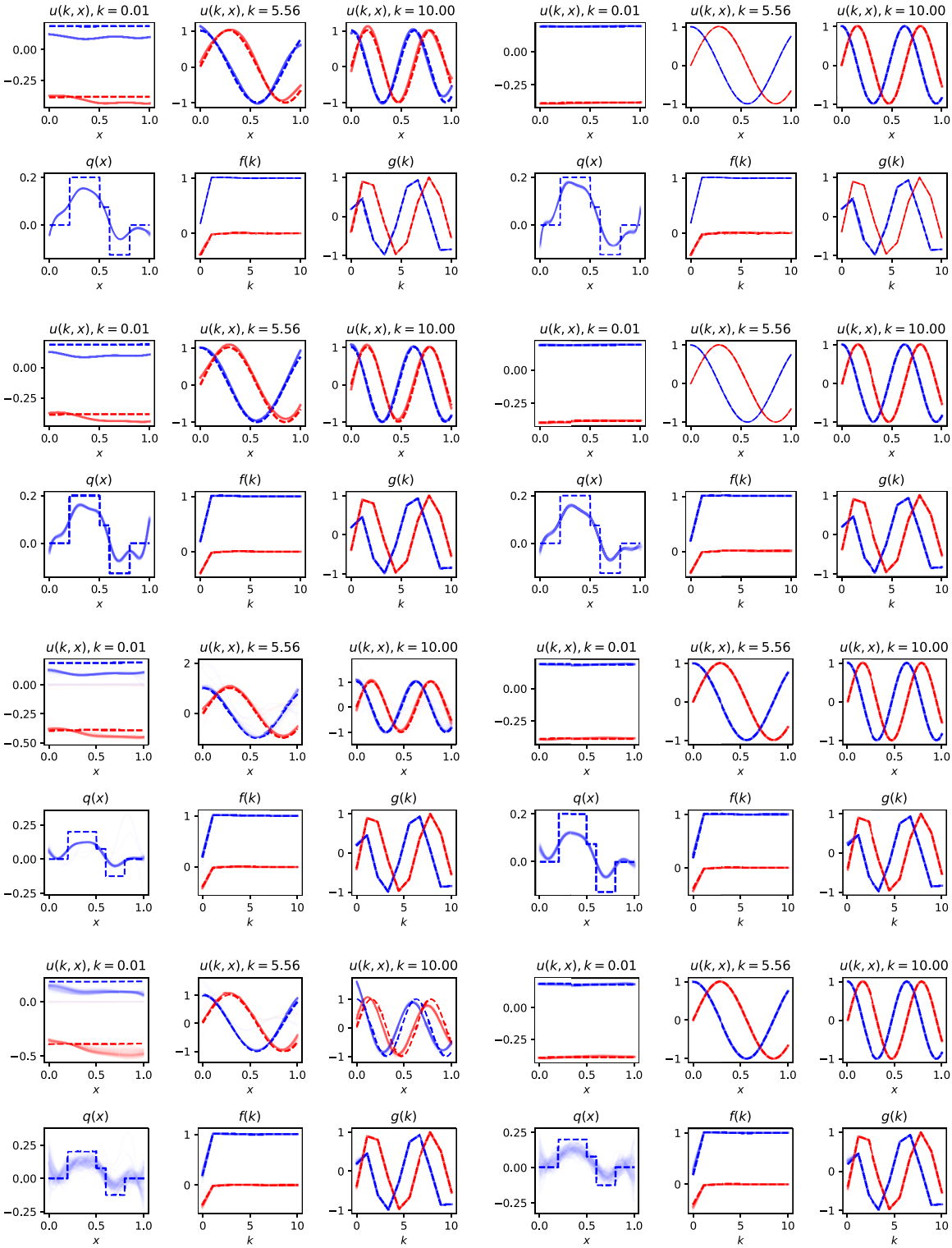

FIG. 6. Results for the LO (left) and DA (right) methods for varying noise levels ($\sigma = 10^{-6}, 10^{-5}, 10^{-4}, 10^{-3}$, respectively, from top to bottom). The subplots follow the same layout as the previous figures. Individual results for different realizations of the noise are superimposed to clearly show the variation.

V. DISCUSSION AND CONCLUSION

We treat the inverse problem of retrieving the scattering potential in a 1D Schrödinger equation from boundary data. To do this, we propose a two-step approach inspired by a previously published ROM-based method. We extend this method, previously applied to 1D diffusion problems with Neumann boundary conditions, to the 1D Schrödinger equation with impedance boundary conditions. In particular, we presented explicit expressions for retrieving the ROM matrices from boundary data and proposed a novel approach for approximating the state from these matrices. This approach, based on ideas from data assimilation, is an alternative to the previously proposed method based on Lanczos orthogonalization. Given the estimates of the states, the scattering potential is obtained by solving an integral equation.

We compared the two approaches numerically on a simulated example with varying noise levels. These experiments suggest that the data-assimilation approach for estimating the state is more accurate and stable and leads to a more stable estimate of the scattering potential for moderate noise levels.

This work is the first step toward extending the ROM-based approach to frequency-domain wave-like problems (e.g., the Helmholtz equation) and 2D/3D. Our numerical experiments are idealized as we have allowed ourselves to compute the optimal values of the required regularization parameters. In practice, one would need to resort to one of the many available parameter estimation methods (e.g., the L-curve method, discrepancy principle, or cross validation). It is not clear if the observed benefits of the DA method remain if the parameters are not carefully tuned. Other open questions for further research include the approximation error, stability estimates, and more practical aspects such as an iterative approach where the reference potential is iteratively updated.

ACKNOWLEDGMENTS

This work was supported by the Utrecht Consortium for Subsurface Imaging (UCSI).

AUTHOR DECLARATIONS

Conflict of Interest

The authors have no conflicts to disclose.

Author Contributions

Tristan van Leeuwen: Conceptualization (equal); Formal analysis (supporting); Funding acquisition (lead); Investigation (equal); Methodology (equal); Software (equal); Supervision (lead); Writing – original draft (equal); Writing – review & editing (equal). **Andreas Tataris**: Conceptualization (equal); Formal analysis (equal); Investigation (equal); Methodology (equal); Software (equal); Writing – original draft (equal); Writing – review & editing (equal).

DATA AVAILABILITY

Data sharing is not applicable to this article as no new data were created or analyzed in this study.

APPENDIX A: PROOFS

Proof of Lemma 1. From the weak form, we find

$$S_{ij} - k_j^2 M_{ij} - \imath k_j B_{ij} = -2\imath k_j \bar{f}_i$$

and

$$S_{ji} - k_i^2 M_{ji} - \imath k_i B_{ji} = -2\imath k_i \bar{f}_j,$$

from which (by taking the conjugate transpose and using the fact that the matrices involved are Hermitian)

$$S_{ij} - k_i^2 M_{ij} + \imath k_i B_{ij} = 2\imath k_i f_j.$$

Combining these yields

$$(k_i^2 - k_j^2) M_{ij} - \imath(k_i + k_j) B_{ij} = -2\imath(k_i f_j + k_j \bar{f}_i)$$

and

$$(k_i^2 - k_j^2) S_{ij} - \imath(k_j^2 k_i + k_i^2 k_j) B_{ij} = -2\imath(k_j^2 k_i f_j + k_i^2 k_j \bar{f}_i),$$

from which, we can compute M_{ij} and S_{ij},

$$M_{ij} = \imath\left(\frac{B_{ij}}{k_i - k_j} - 2\frac{k_i f_j + k_j \bar{f}_i}{k_i^2 - k_j^2}\right),$$

$$S_{ij} = \imath\left(\frac{k_i k_j B_{ij}}{k_i - k_j} - 2\frac{k_j^2 k_i f_j + k_i^2 k_j \bar{f}_i}{k_i^2 - k_j^2}\right).$$

For the diagonal elements, we need to take a limit of the above two relations. We first compute the diagonal elements of M. We set $\lambda = k_j^2$ and $k_i^2 = \lambda + h$. We also define $f(k_j) = \phi(\lambda) = \phi_1 + \imath\phi_2$ and $\phi(\lambda + h) = \phi_1^h + \imath\phi_2^h$ and, similarly, $\gamma(\lambda) = g(k_j)$. Since $\Im(M_{jj}) = 0$, we obtain

$$\begin{aligned} M_{jj} = \lim_{h\to 0} \Bigg\{ & -2\frac{\sqrt{\lambda}\phi_2^h - \sqrt{\lambda+h}\phi_2}{h} \\ & - \frac{\gamma_2\gamma_1^h - \gamma_1\gamma_2^h + \phi_2\phi_1^h - \phi_1\phi_2^h}{\sqrt{\lambda+h} - \sqrt{\lambda}} \Bigg\} \\ = & -2\left(\sqrt{\lambda}\frac{d\phi_2}{d\lambda}(\lambda) - \frac{1}{2}\lambda^{-1/2}\phi_2(\lambda)\right) - \gamma_2(\lambda)2\sqrt{\lambda}\frac{d\gamma_1}{d\lambda}(\lambda) \\ & + \gamma_1(\lambda)2\sqrt{\lambda}\frac{d\gamma_2(\lambda)}{d\lambda} - \phi_2(\lambda)2\sqrt{\lambda}\frac{d\phi_1}{d\lambda}(\lambda) \\ & + \phi_1(\lambda)2\sqrt{\lambda}\frac{d\phi_2(\lambda)}{d\lambda}. \end{aligned} \tag{A1}$$

The product rule gives that $\frac{d\phi}{d\lambda} = \frac{df}{dk}\frac{dk}{dk^2} = f'(k)(2k)^{-1}$ similarly for γ. Combining gives

$$\begin{aligned} M_{jj} = \Bigg\{ & -2\left(k\frac{1}{2k}\Im(f') - \frac{1}{2k}\Im(f)\right) - \Im(g)2k\frac{1}{2k}\Re(g) + \Re(g)2k \\ & \times \frac{1}{2k}\Im(g) - \Im(f)2k\frac{1}{2k}\Re(f) + \Re(f)2k\frac{1}{2k}\Im(f)\Bigg\}\Bigg|_{k=k_j}, \end{aligned}$$

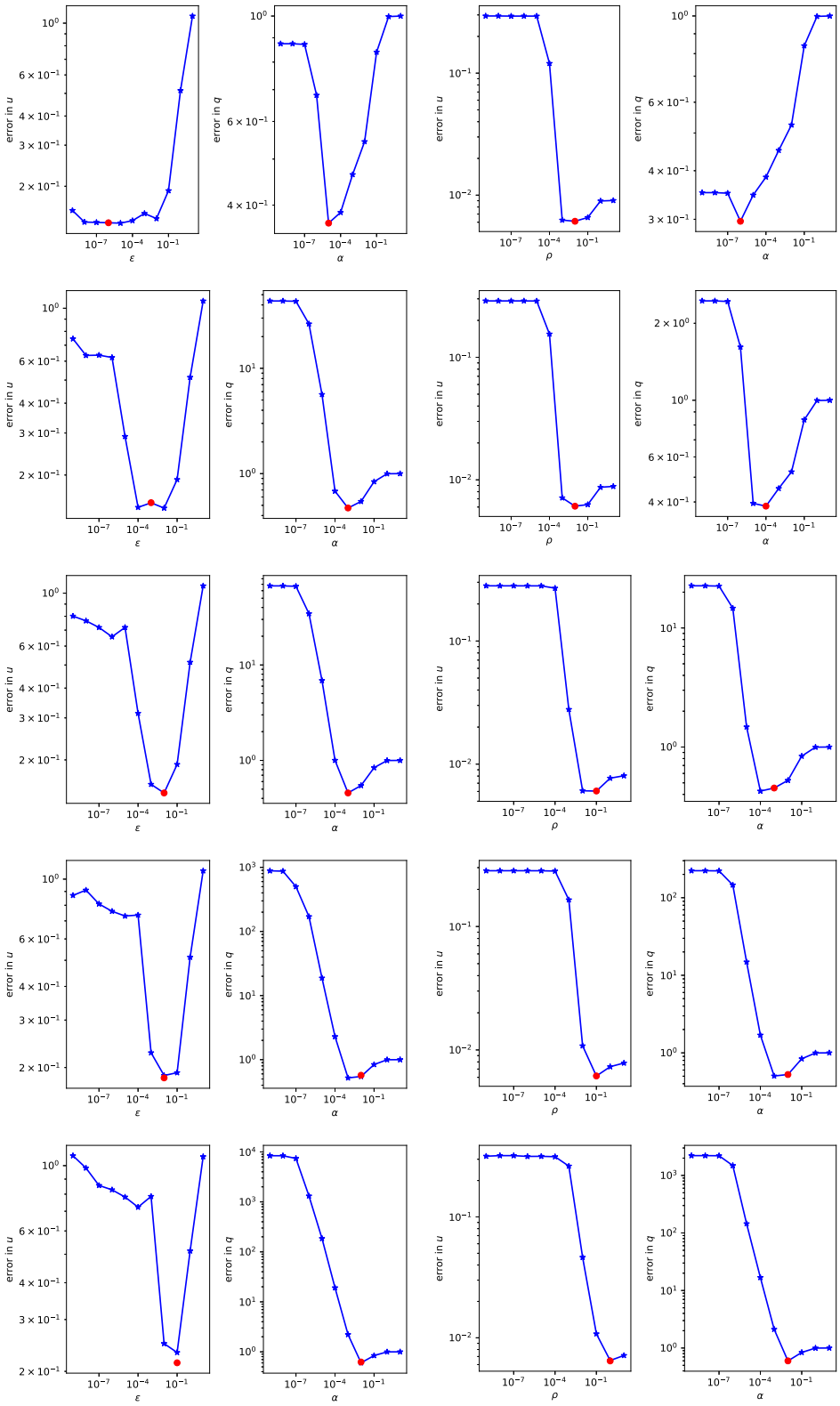

FIG. 7. Average error for both methods (LO, left and DA, right) for various noise levels $(0, 10^{-6}, 10^{-5}, 10^{-4}, 10^{-3}$, respectively, from top to bottom).

which gives

$$M_{jj} = \Re(f_j)\Im(f_j') - \Im(f_j)\Re(f_j') + \Re(g_j)\Im(g_j') - \Im(g_j)\Re(g_j') - \Im(f_j') + \Im(f_j)/k_j.$$

We obtain similarly the relation for the diagonal of S. □

APPENDIX B: REGULARIZATION PARAMETER SELECTION

The LO and DA methods both have two regularization parameters that regularize the problem. For the current experiments, these parameters are chosen to minimize the expected reconstruction error for the given noise level. We approximate the expected error by averaging the error over 100 realizations of the noise. The plots corresponding to the results presented in Table I and Figs. 4–6 are shown in Fig. 7.

Obviously, this procedure can only be applied if the ground truth is known and is chosen here to provide a best-case comparison of the methods. In practice, one would result to data-driven or heuristic methods, such as the discrepancy principle, the L-curve method, or generalized cross validation,[18] to select appropriate values for the parameters.

REFERENCES

[1] E. R. Pike and P. C. Sabatier, *Scattering, Two-Volume Set: Scattering and Inverse Scattering in Pure and Applied Science* (Elsevier, 2001).
[2] J. A. Ware and K. Aki, "Continuous and discrete inverse-scattering problems in a stratified elastic medium. I. Plane waves at normal incidence," J. Acoust. Soc. Am. **45**, 911–921 (1969).
[3] A. Tarantola, "Inversion of seismic reflection data in the acoustic approximation," Geophysics **49**, 1259–1266 (1984).
[4] J. Virieux and S. Operto, "An overview of full-waveform inversion in exploration geophysics," Geophysics **74**, WCC1–WCC26 (2009).
[5] J. Virieux, A. Asnaashari, R. Brossier, L. Métivier, A. Ribodetti, and W. Zhou, "An introduction to full waveform inversion," in *Encyclopedia of Exploration Geophysics* (Society of Exploration Geophysicists, 2017), p. R1–1.
[6] F. Broggini and R. Snieder, "Connection of scattering principles: A visual and mathematical tour," Eur. J. Phys. **33**, 593–613 (2012).
[7] A. Tataris and T. van Leeuwen, "A distributional Gelfand–Levitan–Marchenko equation for the Helmholtz scattering problem on the line," J. Math. Phys. **63**, 103507 (2022).
[8] L. Diekmann, I. Vasconcelos, and T. van Leeuwen, "A note on Marchenko-linearised full waveform inversion for imaging," Geophys. J. Int. **234**, 228–242 (2023).
[9] V. Druskin, S. Moskow, and M. Zaslavsky, "Lippmann–Schwinger–Lanczos algorithm for inverse scattering problems," Inverse Probl. **37**, 075003 (2021).
[10] L. Borcea, J. Garnier, A. V. Mamonov, and J. T. Zimmerling, "Reduced order model approach for imaging with waves," Inverse Probl. **38**, 025004 (2021).
[11] R. Kress, *Linear Integral Equations* (Springer, 2014), Vol. 82.
[12] J. P. Fink and W. C. Rheinboldt, "On the error behavior of the reduced basis technique for nonlinear finite element approximations," Z. Angew. Math. Mech. **63**, 21–28 (1983).
[13] Y. Maday, A. T. Patera, and G. Turinici, "A priori convergence theory for reduced-basis approximations of single-parameter elliptic partial differential equations," J. Sci. Comput. **17**, 437–446 (2002).
[14] K. Veroy, C. Prud'Homme, D. Rovas, and A. Patera, "*A posteriori error bounds for reduced-basis approximation of parametrized noncoercive and nonlinear elliptic partial differential equations*," in *16th AIAA Computational Fluid Dynamics Conference* (AIAA, 2003), p. 3847.
[15] S. Sen, K. Veroy, D. B. P. Huynh, S. Deparis, N. C. Nguyen, and A. T. Patera, "'Natural norm' a posteriori error estimators for reduced basis approximations," J. Comput. Phys. **217**, 37–62 (2006).
[16] T. v. Leeuwen and F. J. Herrmann, "A penalty method for PDE-constrained optimization in inverse problems," Inverse Probl. **32**, 015007 (2015).
[17] A. Tataris and T. van Leeuwen, "A regularised total least squares approach for 1D inverse scattering," Mathematics **10**, 216 (2022).
[18] C. R. Vogel, *Computational Methods for Inverse Problems* (SIAM, 2002).